DOI 10.1007/s10812-018-0682-9
Journal of Applied Spectroscopy, Vol. 85, No. 3, July, 2018 (Russian Original Vol. 85, No. 3, May–June, 2018)

FT-IR AND RAMAN SPECTROSCOPY AND COMPUTATION OF 5-METHYLFURFURAL

Y. Erdogdu,[a*] T. R. Sertbakan,[b] M. T. Güllüoğlu,[c] Ş. Yurdakul,[a] and A. Güvenir[b]

UDC 535.375.5;535.34

5-Methylfurfural (5MF) was studied by vibrational (IR and Raman) spectroscopy and computational methods (DFT/B3LYP&MP2). FT-IR and FT-Raman spectra in KBr (at room temperature) were collected. The Gaussian 09 and Spartan 08 programs were used for conformational analysis and calculations of molecular structure, torsional barrier, and vibrational spectral data for the 5MF molecule. The obtained results were used in the analysis of experimental vibrational spectra of 5MF molecule.

Keywords: *5-methylfurfural, DFT/B3LYP, MP2, FT-IR and FT-Raman spectra.*

Introduction. One of the reasons for the rapid development of clean renewable energy is the energy crisis. There are many possible solutions for the energy crisis. One of them is the effective use of renewable energy sources. Renewable energy sources such as solar, wind, biomass, etc. can solve the energy crisis. They are widespread, clean, and renewable. Especially biomass resources have the potential to serve as a sustainable supply of fuels and chemical intermediates [1]. Research on conversion of biomass to a platform for the chemicals supply has received much attention. Chheda et al. [2] reported that the challenge for the effective utilization of these sustainable resources is to develop cost-effective methods to transform highly functionalized carbohydrate moieties into value-added chemicals.

The cellulose in biomass can be transformed into some chemicals such as hexoses, furfural, levulinic acid, ethanol, and biopolymers. One of the important results is the energy structure conversion. Another important result is environment improvement [3]. Biomass-derived molecules are a promising class of alternative energy resources to produce fuels and chemicals [4]. These molecules generally contain more oxygen atoms than the ones found in petroleum-based feedstock, and the nature of oxygen over functionalization plays a major barrier for the efficient utilization of biomass [5]. Controlling the activity and selectivity of the hydrodeoxygenation (HDO) reaction is critical for the upgrading of biomass feed stocks. An important example of the chemical group is furan and its derivatives. For example, furfural and 5-hydroxymethylfurfural can be manufactured from renewable biomass resources. As a result of hydrolysis and dehydration of xylose from hemicellulose, furfural compounds were obtained by Bicker et al. [6]. These compounds have the potential to be sustainable substitutes for building blocks derived from petrochemicals in the production of plastics and fine chemicals [7]. Furfural has several carbon-oxygen bonds in the furan ring. Therefore, this compound is a model compound of biomass derivatives.

There have been numerous studies of internal rotation of furfural. They have been determined in several media through experimental and theoretical methods [8–16]. In these studies, the relative stability of furfural conformations was determined. They have also determined the barrier to internal rotation. Crespo-Otero et al. [17] have shown the effect of substitution (CH_3, NH_2, NO, and F) in furfural on conformational preferences of formyl group by using the MP2/6-31G(p,d) level of theory. Many infrared and Raman spectroscopic data have been found in [10, 15, 18] for furfural molecules. The infrared and Raman spectra of furfural molecule were studied early by Allen and Bernstein [8]. In that study, infrared and Raman spectra were measured photoelectrically in liquid and solution samples. Motiyenko et al. [19] reported on the microwave spectroscopy of furfural in vibrationally excited states. The far-IR spectra of gaseous and solid furfural have been recorded by Little et al. [15]. Additionally, the Raman spectra of the gas and liquid have been obtained at different temperatures. The spectrum of the solid

*To whom correspondence should be addressed.

[a]Gazi University, Faculty of Science, Department of Physics, Ankara, Turkey; e-mail: yusuferdogdu@gmail.com; [b]Ahi Evran University, Faculty of Art and Science, Department of Physics, Kirsehir, Turkey; [c]Harran University, Sanliurfa, Turkey. Abstract of article is published in Zhurnal Prikladnoi Spektroskopii, Vol. 85, No. 3, p. 512, May–June, 2018.

at 25 K has been obtained in that study. In this study, our goal is to combine the experimental results with quantum chemical calculations and to evaluate IR and Raman spectra of the 5MF molecule. Thus, the main aim of this work was to obtain the characteristic spectral features of structural parts of 5MF. The study of substituted furfural helps further developments and increases expectations for future applications of these compounds.

Experimental. 5-Methylfurfural from Sigma-Aldrich Chemical Company with a stated purity 99% was used without further purification. FT-IR spectra were measured in the Bruker IFS 66 v/S instrument as a KBr disc. The resolution of the FT-IR instrument was 2 cm^{-1}. Each spectrum was accumulated by acquisition of 64 scans. The FT-IR spectrum was recorded in the range of 4000–400 cm^{-1}. The Raman spectrum was measured in the range of 3500–50 cm^{-1} on a Bruker FRA-106/S instrument operating at the 1064 nm exciting line of Nd:YAG laser. The resolution of FT-Raman instrument was 2 cm^{-1}. The spectrum was accumulated by acquisition of 200 scans.

Calculation. Conformational distributions of the 5MF molecule obtained by scanning the potential energy surface were determined using the Spartan 08 program [20]. To do this, the Merck molecular force field (MMFF) [21] method was used. After determining all conformations to identify the most stable conformation, all calculations were performed at the DFT/B3LYP computational level by using the Gaussian 09W A 02 program and Gauss View 5.0.9 molecular visualization program package [22, 23]. Since the furan and aldehyde groups can be rotated to around the C–C bonds, we also determined the torsional potential energy surface. The torsional potential energy surface was calculated changing the O_{11}–C_2–C_9–O_{10} dihedral angle. The surface was scanned in the full range of rotation, 0–180°. The rotation step was 10° for the aldehyde group.

The calculations employed *ab initio* MP2 and the B3LYP exchange–correlation functional, which combines the hybrid exchange functional of Becke [24–26] with the gradient-correlation functional of Lee et al. [27] and the split-valence basis set (6-311G(d,p)) [28]. The obtained data showed that DFT calculation results are in better agreement with the experimental data [29, 30]. Potential energy distribution (PED) calculations were performed by the scaled quantum mechanical (SQM) method [31, 32] using the output files created at the end of the frequency calculations. The theoretical Raman intensities of computed normal modes were calculated by using the RaInt program [33]. In addition, the GaussView 5.0.9 was used for visualization of the optimized molecular structures, MESP surface, and the shape of HOMO and LUMO orbitals.

Results and Discussion. *Potential energy barrier.* The starting point for further calculations is to determine the most stable conformer for molecule under investigation. The only bond around which rotation is permitted is the C–C bond, which acts as interlink between the furan ring and aldehyde. Torsional potential energy was computed as a function of angle of rotation around the C–C bond, in steps of 10° between 0° and 180°. The results are shown graphically in Fig. 1. In this figure, it can be seen that the *cis*- and *trans*-isomers occurs at the rotation angle of 0° and 180°, respectively. Hence, the *trans*-rotamer was determined for the global minimum geometry. Relative energy of the *cis*-rotamer was calculated at 0.973 kcal/mol. Relative energy of the transition state, which is perpendicular rotamer, was predicted at 14.72 kcal/mol. The optimized energy of the *cis*-rotamer is slightly larger than that of *trans*-rotamer. However, further calculations were performed with these optimized structures (*trans* and *cis*) shown in Fig. 1.

Molecular geometry. The molecular structures along with numbering of atoms of the 5MF are shown in Fig. 1. The optimized structural parameters of the 5MF are shown in Table 1 for *cis*- and *trans*-rotamers. To the best of our knowledge, no X-ray crystallographic data of the 5MF molecule have been established. Optimized geometrical parameters of the 5MF were compared with those of 5-(hydroxymethyl)furan-2-carbaldehyde [34]. The optimized structural parameters of the *trans*- and *cis*-rotamers are very close together in the B3LYP calculation. A closer agreement was also obtained between predicted structural parameters of the rotamers and those determined for 5-(hydroxymethyl)furan-2-carbaldehyde.

Vibrational assignments. The 5MF molecule has 14 atoms. It possesses 36 normal modes of vibrations. The symmetry of the molecular structures as shown in Fig. 1 corresponds to the C_S point group. All the vibrations are active in the infrared and Raman spectra. Usually the calculated harmonic vibrational wavenumbers are higher than the experimental ones due to the anharmonicity of the incomplete treatment of electron correlation and the use of finite one-particle basis set. In our study, the harmonic frequencies were calculated at the B3LYP/6-311G(d,p) and MP2/6-311G(d,p) levels of theory and then scaled by 0.967 and 0.960, respectively. Assignments of infrared frequencies were achieved by comparing the band positions and intensities observed in IR spectra with wavenumbers and intensities from molecular modeling calculations. The FT-IR and FT-Raman spectra of the 5MF are given in Fig. 2. Experimentally observed and theoretically calculated harmonic vibrational frequencies are shown in Table 2.

In the region from 3000 to 3100 cm^{-1}, C–H stretching vibration modes are present and the aromatic rings generally show their characteristic bands. In the furan ring, the 3121-cm^{-1} peak was measured in the FT-IR spectra as a CH stretching vibration. This peak was calculated at 3137 (B3LYP) and 3120 cm^{-1} (MP2) for the *trans* rotational isomer (*trans*-rotamer).

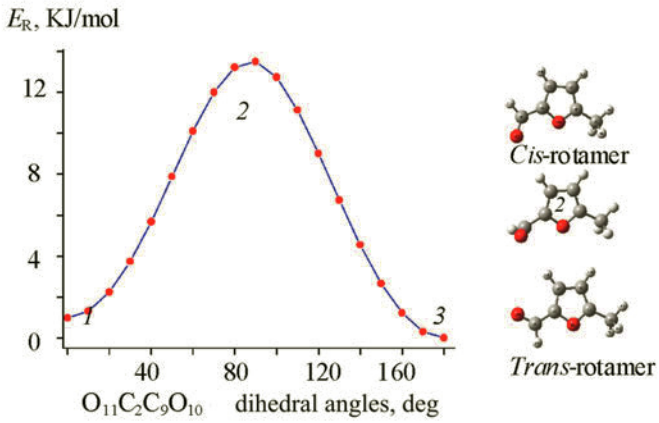

Fig. 1. Torsional potential energy surface of 5MF at the B3LYP/6311G(d,p) level of theory.

TABLE 1. The Optimized Structural Parameters of *cis*- and *trans*-Rotamers

B3LYP/6-311G(d,p)							
	Bond lengths, Å		X-Ray [35]		Bond angles, deg		X-Ray [34]
	cis	*trans*			*cis*	*trans*	
C_1–C_2	1.371	1.369	1.364	C_2–C_1–C_4	106.5	106.4	106.2
C_1–C_4	1.420	1.419	1.422	C_2–C_1–H_{13}	125.8	125.1	126.8
C_1–H_{13}	1.079	1.078	0.950	C_4–C_1–H_{13}	127.5	128.3	126.8
C_2–C_9	1.452	1.453	1.443	C_1–C_2–C_9	130.8	133.0	129.9
C_2–O_{11}	1.370	1.376	1.377	C_1–C_2–O_{11}	109.4	109.4	110.3
C_3–C_4	1.370	1.370	1.356	C_9–C_2–O_{11}	119.6	117.4	119.6
C_3–C_5	1.485	1.485	–	C_4–C_3–C_5	133.0	133.1	–
C_3–O_{11}	1.355	1.356	1.370	C_4–C_3–O_{11}	110.1	109.8	110.7
C_4–H_{12}	1.078	1.078	0.951	C_5–C_3–O_{11}	116.8	116.9	–
C_5–H_6	1.093	1.094	–	C_1–C_4–C_3	106.3	106.7	106.6
C_5–H_7	1.093	1.094	–	C_1–C_4–H_{12}	127.5	127.4	126.6
C_5–H_8	1.090	1.090	–	C_3–C_4–H_{12}	126.0	125.8	126.6
C_9–O_{10}	1.211	1.213	1.219	C_3–C_5–H_6	110.8	111.0	–
C_9–H_{14}	1.111	1.109	0.950	C_3–C_5–H_7	110.8	111.0	–
				C_3–C_5–H_8	110.1	110.0	–
				H_6–C_5–H_7	107.5	107.5	–
				H_6–C_5–H_8	108.6	108.5	–
				H_7–C_5–H_8	108.6	108.5	–
				C_2–C_9–O_{10}	125.7	123.9	125.6
				C_2–C_9–H_{14}	112.4	114.0	117.1
				O_{10}–C_9–H_{14}	121.8	122.0	117.1
				C_2–O_{11}–C_3	107.4	107.4	

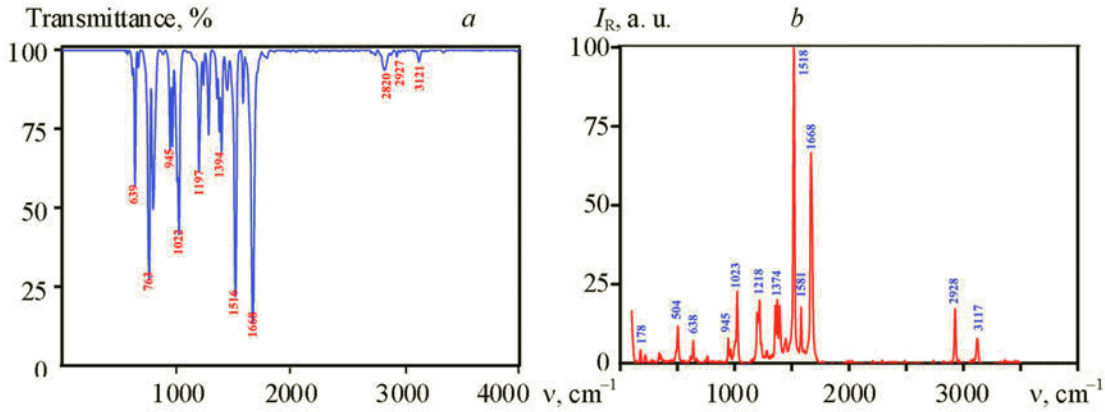

Fig. 2. Experimental FT-IR (a) and FT-Raman (b) spectra of 5MF.

The CH stretching vibration of the *cis* rotational isomer (*cis*-rotamer) was determined at 3133 (B3LYP) and 3115 cm^{-1} (MP2). Allen and Bernstein [8] reported that the CH stretching mode of furfural molecule was observed at ~3140 and ~3090 cm^{-1} for the *trans*- and *cis*-rotamer in the IR spectrum of the liquid form. In our results, it was realized that there was a small shift (4 cm^{-1}) for the CH stretching vibration of 5MF at the B3LYP/6-311G(d,p) level of theory. But Allen et al. [8] reported that the C–H stretching mode of the furfural was shifted to the nearest aldehyde group. The C–H in-plane bending vibrations appear in the region 1000–1520 cm^{-1} and the C–H out-of-plane bending vibrations appear in the range of 700–1000 cm^{-1} [35, 36]. Calculated modes at 1008 and 1189 cm^{-1} were assigned to the in-plane CH bending vibrations. These calculated modes give a more than 40% contribution to the C–C stretching mode. The corresponding mode was observed as a strong band in the FT-IR spectra at 1197 cm^{-1}. Calculated mode at 1008 cm^{-1} vibration could not be detected in the FT-IR and FT-Raman spectra. The strong band at 797 cm^{-1} (FT-IR) was identified as the out-of-plane CH bending mode of the furan ring (mode No: 12). This mode was predicted at 793 and 756 cm^{-1} (B3LYP and MP2) in the *trans*-rotamer. The calculated vibrations at 870 and 782 cm^{-1} (B3LYP and MP2) were assigned to the out-of-plane CH bending vibration (mode No. 13) in the *trans*-rotamer. Nevertheless, this peak was not observed in either of the spectra. The in-plane and out-of-plane bending of the furan ring appear as mixed vibrations of methyl and aldehyde group, ring bending vibrations with considerable PED values. The C–O stretching [37] vibrations are expected in the region 1190–1050 cm^{-1}, and in the present study C–O vibrations in furan rings appear at 1197 cm^{-1}. The B3LYP calculations give this mode at 1200 (*cis*-rotamer) and 1189 cm^{-1} (*trans*-rotamer) mode No. 21 and its PED contributions 26% and 36%, respectively. In the *trans*-rotamer, the C–C stretch mode of the furan ring is theoretically predicted at 1501 cm^{-1} (1505 cm^{-1} *cis*-rotamer) and 1572 cm^{-1} (1568 cm^{-1} *cis*-rotamer) at the B3LYP/6-311 G(d,p) level of theory. These vibrational bands experimentally appear at 1516 (ms) and 1584 cm^{-1} (w) in the IR and at 1518 (vs) and 1581 cm^{-1} (s) in the Raman spectra. From PED data, it can be noticed that most of the calculated modes give a 35% contribution to the C–C stretching mode.

The aldehyde C–H stretching vibration can be distinctly observed in both IR and Raman spectra by its band position in the low-wavenumber region, compared to other C–H stretching vibrations. On the other hand, the 2820 cm^{-1} band is assigned to the CH stretching vibration of the aldehyde group in the infrared spectra. This band was predicted at 2786 cm^{-1} for the *cis*-rotamer and 2811 cm^{-1} for the *trans*-rotamer at the B3LYP/6-311G(d,p) level of theory. Allen and Bernstein [8] measured the band at 2856 cm^{-1} for the *cis*-rotamer and 2814 cm^{-1} for the *trans*-rotamer. Our calculation predicted that CH stretching of the aldehyde group of the *trans*-rotamer is larger than that of the *cis*-rotamer. Kim et al. [38] reported that CH stretching vibration was predicted at 2920 cm^{-1} for the *cis*-rotamer. Iliescu et al. [39] reported that CH stretching vibration of the 5-(4-fluor-phenyl)-furan-2-carbaldehyde molecule recorded at 2853 cm^{-1} in the FT-IR spectra and 2854 cm^{-1} in the FT-Raman spectra as weak and medium bands, respectively. In that study, it was predicted at 2854 cm^{-1} for the *trans*-rotamer and 2815 cm^{-1} for the *cis*-rotamer by using DFT. In-plane CH bending vibrations of the aldehyde group, mode No. 25, was detected at 1375/1374 cm^{-1} (FT-IR/FT-Raman), and mode No. 23 was detected at 1335 cm^{-1}(FT-Raman). According to the PED result, PED contribution of the mode No. 25 was predicted at 55% (*trans*-rotamer) and 41% (*cis*-rotamer). PED contribution of the other vibrations was smaller than that of in-plane CH bending vibration. Mode no: 25 almost predicted the pure in-plane CH bending. Out-of-plane bending vibration of the aldehyde group was calculated at 988 and 973 cm^{-1} for B3LYP and MP2, respectively. It is could not be detected in the FT-IR and FT-Raman spectra. PED contribution of this

TABLE 2. Detailed Vibrational Assignments of Rotamers of 5-Methylfurfural along with Potential Energy Distribution

cis		B3LYP			MP2	PED	*trans*	B3LYP			MP2	PED	Experimental	
		ν [a]	I_{IR}	I_{Raman}	ν [a]			ν[a]	I_{IR}	I_{Raman}	ν [a]		FT-IR	FT-Raman
ν_3	*A'*	160	1.680	23.55	155	$38\delta_{CCO} + 37\delta_{CCC}$	*A'*	172	1.171	2.488	166	$36\delta_{CCO} + 20\delta_{CCH} + 25\delta_{CCC}$	–	178 vw
ν_4	*A"*	198	3.575	25.01	187	$27\tau_{CCCC} + 17\tau_{CCCO} + 16\tau_{CCOC} + 16\tau_{OCCH}$	*A"*	243	6.343	3.201	223	$33\tau_{CCCH} + 15\tau_{CCCO} + 10\tau_{CCOC}$	–	221 vw
ν_6	*A'*	340	0.429	5.277	329	$29\delta_{CCO} + 27\delta_{CCC} + 15\delta_{CCH}$	*A'*	324	2.372	13.21	314	$27\delta_{CCO} + 22\delta_{CCC} + 21\delta_{CCH}$	–	341 vw
ν_7	*A'*	486	0.095	26.64	474	$36\delta_{CCO} + 28\delta_{CCC} + 21\nu_{CC}$	*A'*	473	0.052	10.42	464	$27\delta_{CCO} + 18\delta_{CCH} + 16\delta_{CCC} + 14\nu_{CC}$	–	504 w
ν_8	*A"*	613	0.054	0.126	544	$32\tau_{CCCH} + 25\tau_{CCCO} + 20\tau_{CCCC} + 12\tau_{CCOC}$	*A"*	613	0.277	0.055	535	$38\tau_{CCCH} + 15\tau_{CCCO} + 11\tau_{OCCH}$	617 vw	613 vw
ν_9	*A'*	628	3.684	14.30	617	$36\nu_{C–CH3} + 31\delta_{CCH} + 30\delta_{CCO}$	*A"*	630	0.019	2.171	608	$27\tau_{CCCH} + 18\tau_{OCCH} + 16\tau_{CCOC}$	639 s	638 w
ν_{10}	*A"*	637	0.046	5.486	620	$23\tau_{CCCO} + 17\tau_{OCCH} + 17\tau_{CCCH} + 17\tau_{CCOC}$	*A'*	652	1.764	4.849	641	$38\nu_{C–CH3} + 24\delta_{CCO} + 19\delta_{CCH}$	668 vw	–
ν_{11}	*A'*	750	15.21	0.370	737	$32\delta_{CCC} + 29\delta_{CCO} + 11\nu_{CC}$	*A'*	742	22.68	4.570	727	$25\delta_{CCH} + 23\delta_{CCO} + 17\nu_{CC} + 17\delta_{CCC}$	763 ms	764 vw
ν_{12}	*A"*	783	13.24	0.033	748	$64\gamma_{CCH} + 18\tau_{HCCH}$	*A"*	793	13.86	0.064	756	$82\gamma_{CCH} + 24\tau_{HCCH}$	797 s	–
ν_{14}	*A'*	931	2.579	5.389	920	$30\delta_{CCH} + 19\delta_{CCC} + 10\tau_{OCCH} + 10\delta_{CCO}$	*A'*	939	0.886	1.120	927	$36\delta_{CCH} + 10\delta_{CCC} + 10\tau_{OCCH}$	945 s	945 w
ν_{15}	*A'*	961	1.344	7.739	941	$36\delta_{CCC} + 18\nu_{CC} + 16\delta_{CCO} + 13\nu_{CO}$	*A'*	959	1.789	3.896	940	$39\delta_{CCH} + 13\delta_{CCO} + 12\nu_{CC} + 10\nu_{CO}$	966 s	965 vw
ν_{18}	*A'*	1011	14.01	14.47	1000	$59\delta_{CCH} + 15\nu_{CC}$	*A'*	1008	10.64	12.69	998	$52\delta_{CCH} + 13\nu_{CC} + 12\tau_{CCCH}$	1008 vw	
ν_{19}	*A"*	1028	0.957	0.011	1016	$37\delta_{HCH} + 18\Gamma_{CCCC} + 18\tau_{OCCH} + 10\tau_{CCOC}$	*A"*	1028	0.995	0.049	1015	$46\delta_{HCH} + 19\tau_{OCCH} + 10\tau_{CCOC}$	1022 s	1023 s
ν_{21}	*A'*	1200	3.150	17.35	1233	$31\delta_{CCC} + 15\nu_{CC} + 15\nu_{CO} + 10\delta_{CCH}$	*A'*	1189	15.25	8.596	1221	$47\delta_{CCH} + 17\nu_{CC} + 10\delta_{CCO}$	1197 s	1195 vw
ν_{22}	*A'*	1253	8.478	9.849	1271	$34\delta_{CCH} + 26\nu_{CC} + 11\nu_{CO} + 11\delta_{CCO}$	*A'*	1221	8.766	10.31	1234	$33\delta_{CCH} + 21\nu_{CC} + 14\delta_{CCO} + 11\nu_{CO}$	1236 w	1218 s
ν_{24}	*A'*	1366	2.995	8.911	1354	$48\delta_{HCH} + 24\delta_{CCH}$	*A'*	1370	0.914	5.929	1357	$75\delta_{HCH} + 10\nu_{CC}$	1355 vw	1355 vw
ν_{25}	*A'*	1382	4.919	9.094	1370	$30\nu_{CC} + 23\delta_{CCH} + 13\delta_{HCH}$	*A'*	1383	6.175	7.899	1375	$40\delta_{CCH} + 13\delta_{OCH} + 11\delta_{HCH} + 10\nu_{CC}$	1375 s	1374 s
ν_{26}	*A"*	1424	2.486	7.991	1417	$85\delta_{HCH} + 10\delta_{CCH}$	*A"*	1426	2.969	5.090	1418	$85\delta_{HCH} + 10\delta_{CCH}$	1394 s	1393 ms
ν_{27}	*A'*	1441	3.141	19.911	1438	$64\delta_{HCH} + 21\delta_{CCH}$	*A'*	1441	2.314	11.61	1439	$55\delta_{HCH} + 17\delta_{CCH}$	1444 vw	1446 vw
ν_{28}	*A'*	1505	38.29	100	1483	$32\nu_{CC} + 20\delta_{CCC} + 13\delta_{CCO} + 10\delta_{HCH}$	*A'*	1501	83.13	100	1490	$34\nu_{CC} + 18\delta_{CCH} + 14\delta_{CCO} + 10\delta_{HCH}$	1516 ms	1518 vs
ν_{29}	*A'*	1568	2.553	7.821	1542	$35\delta_{CCC} + 30\nu_{CC} + 11\delta_{CCO}$	*A'*	1572	7.525	2.524	1544	$35\delta_{CCH} + 31\nu_{CC} + 14\delta_{CCO}$	1584 w	1581 s
ν_{30}	*A'*	1711	100	63.97	1670	$26\nu_{CO} + 23\delta_{CCC} + 23\delta_{CCO} + 20\nu_{CC}$	*A'*	1705	100	33.52	1665	$29\nu_{CO} + 19\delta_{CCH} + 14\nu_{CC} + 11\delta_{CCO}$	1668 vs	1668 ms
ν_{31}	*A'*	2786	38.10	26.54	2813	$83\nu_{CH}$	*A'*	2811	36.99	13.96	2834	$80\nu_{CH}$	2820 vw	
ν_{32}	*A'*	2933	4.445	33.11	2927	$90\nu_{CH3}$	*A'*	2931	6.542	22.11	2925	$89\nu_{CH3}$	2927 w	2928 s
ν_{35}	*A'*	3133	0.844	7.540	3115	$82\nu_{CH}$	*A'*	3137	0.833	5.590	3120	$77\nu_{CH}$	3121 vw	3120 m

Note. Relative absorption intensities (I_{IR}) and relative Raman intensities (I_{Raman}) normalized with the highest peak absorption equal to 100; potential energy distribution calculated at the B3LYP/6-311G(d,p) level of theory, only contributions ≥10% are listed; vs: very strong; m: medium; s: strong; w: weak; vw: very weak; ν: stretching; τ: torsion; γ: out-of-plane bending; δ: in-plane bending.

[a]Obtained from the wavenumbers calculated at B3LYP/6-311G(d.p) using scaling factor 0.966 and at MP2/6-311G(d.p) using scaling factor 0.950.

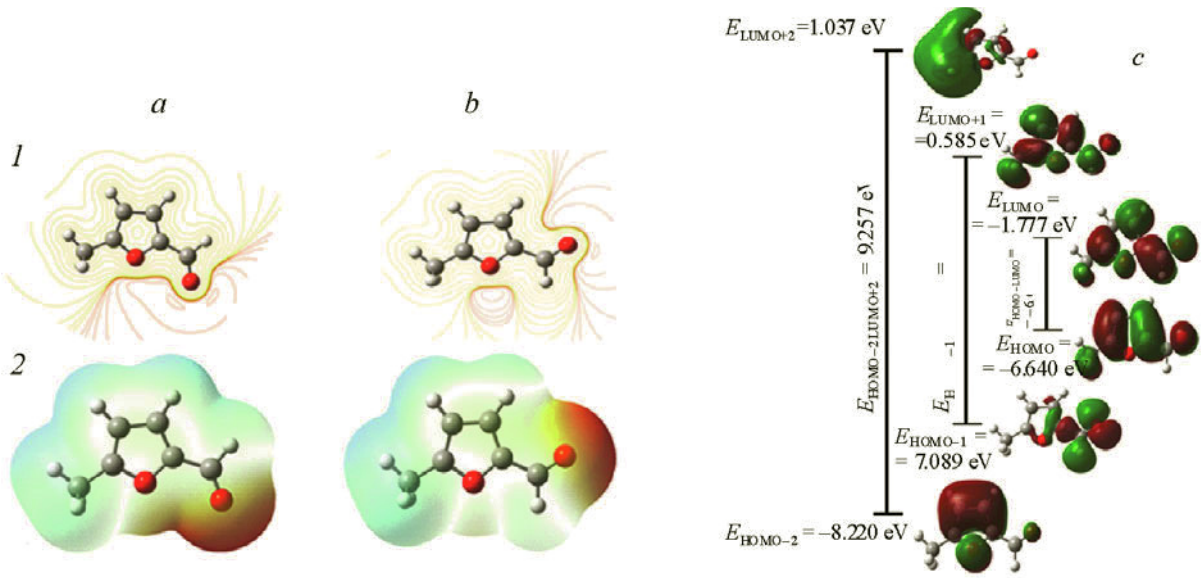

Fig. 3. Electrostatic potential contour (1), electrostatic potential (2) HOMO (a, b) and LUMO (c) plots of 5MF.

vibration was predicted at 35%. According to PED results, other CH bending (in-plane and out-of-plane) vibrations of the aldehyde group were mixed with those of furan and methyl groups.

In the aldehyde group, the CO stretching peak appeared at 1668 cm^{-1} as a very strong band in the FT-IR spectra. In the Raman spectra, this vibration was measured at the same wavenumber as a strong band. The DFT result was assigned at 1705 and 1711 cm^{-1} (*trans*- and *cis*-rotamer) as 30% and 38% of PED contribution, respectively. In the *cis*-rotamer, the CO stretching vibration of the aldehyde group was detected at 1675 and 1676 cm^{-1} in the liquid form by FT-IR and FT-Raman spectra, respectively [8]. Under the same condition, this peak of the *trans*-rotamer was measured at 1695 and 1693 cm^{-1} (FT-IR and FT-Raman) by Allen et al. [8]. While comparing this mode with the experimental one, the CO stretching vibration of the *trans*-rotamer shows good agreement with Allen's experimental results.

The C–H stretching frequencies of the methyl group appear just below 3000 cm^{-1} [40]. The title molecule possesses the methyl ($–CH_3$) group. The strong and distinct C–H stretching bands at 2927 (FT-IR) and at 2928 cm^{-1} (FT-Raman) are in agreement with the theoretical values of 2931 cm^{-1} (mode No. 32) by the B3LYP method and are well supported by the PED values. The asymmetric and symmetric bending vibrations of methyl groups normally appear in the region 1465–1440 and 1390–1370 cm^{-1}, respectively [40]. In the present study, asymmetric CH_3 bending vibration (mode No. 27) was observed at 1444 cm^{-1} in the FT-Raman spectrum as a very weak band and its corresponding counterpart was detected at 1446 cm^{-1} in the FT-IR spectrum. The asymmetric CH_3 bending mode of the methyl group was also predicted at 1441 and 1439 cm^{-1} at the B3LYP and MP2 with 6-311 G(d,p) level of theory, respectively. The 1394 (FT-IR) and 1393 cm^{-1} (FT-Raman) peaks were assigned to the symmetric bending vibration of the CH_3 group. This frequency was calculated at 1424 and 1426 cm^{-1} (*cis*- and *trans*-rotamer) at the B3LYP/6-311 G(d,p) level of theory.

Molecular electrostatic potential. The MEP is related to the electronic density. It is a very useful tool for detecting the region of the electrophilic and nucleophilic reactions and hydrogen bonding interaction [41–43]. The red color regions of MEPs have electrophilic activity. They are the electron-rich sites. The blue colors of them have the nucleophilic reactivity. These sites are poor electron sites. In the MEP map, a red and blue area shows the regions of negative and positive potentials, whereas the green color indicates the neutral electrostatic potential. The MEP surface provides necessary information on the reactive sites. The molecular electrostatic potential (MEP) and electrostatic potential contour maps of 5MF are shown in Fig. 3. As shown in Fig. 3, the red colored regions are over oxygen atom on the furan and aldehyde group. The blue colored regions are over whole hydrogen atoms localized at the maximum positive region. From these results, all hydrogen atoms point out the strongest attraction and oxygen atoms indicate the strongest repulsion.

Frontier molecular orbital analysis. Molecular orbital analysis can provide the reactivity, structural, electronic, and some chemical properties of molecules. The energy of the HOMO orbital shows the ionization potential of the molecules. The energy of the LUMO orbital represents the electron affinity. The HOMO–LUMO gap determines the chemical stability

TABLE 3. Comparison of Some Chemical Reactivity Parameters of the Title Compound

Parameters	*Trans*-rotamer	*Cis*-rotamer
E_{HOMO}, eV	–6.640	–6.683
E_{LUMO}, eV	–1.777	–1.726
ΔE_{HOMO}–ΔE_{LUMO}, eV	4.863	4.957
$E_{HOMO–1}$, eV	–7.089	–7.025
E_{LUMO+1}, eV	0.585	0.700
$\Delta E_{HOMO–1}$–ΔE_{LUMO+1}, eV	7.674	7.725
$E_{HOMO–2}$, eV	–8.220	–8.256
E_{LUMO+2}, eV	1.037	1.052
$\Delta E_{HOMO–2}$–ΔE_{LUMO+2}, eV	9.257	9.308
Ionization potential, eV	6.640	6.683
Electron affinity, eV	1.777	1.726
Electronegativity χ, eV	4.208	4.204
Chemical hardness H, eV	2.431	2.478
Global softness *S*, eV^{-1}	0.205	0.201
Chemical potential μ, eV	–4.208	–4.204
Electrophilicity index Ω, eV	3.641	3.565

and electrical transport properties [44]. If a molecule has a small frontier orbital gap, it is more reactive. It is generally associated with a high chemical reactivity. Also, the lowering of the energy gap shows that the eventual charge transfer takes place within the molecule [45]. The energy of HOMO, LUMO and their orbital energy gap of 5MF were calculated by the B3LYP/6-311G(d,p) method, and they are given in Fig. 3, whereas the red colors of the MO plot represent the positive region, and the green colors show the negative ones. The HOMO–LUMO gap of 5MF calculated at B3LYP/6-311G(d,p) level were calculated at 4.863 and 4.957 eV (*trans* and *cis*) in the gas phase. In accordance with Koopmans' theorem, some chemical parameters of 5MF were also calculated [46]. Electron affinity assigned *EA* is equal to the negative value of LUMO energy ($EA = -E_{LUMO}$), and ionization potential assigned *IP* is equal to the negative value of HOMO energy ($IP = -E_{HOMO}$). Electronegativity (χ), chemical hardness (η), softness (*S*), chemical potential (μ), and electrophilicity index (ω) can be calculated by using HOMO and LUMO energy values for a molecule.

According to the finite difference approximations, *I* and *A* are the ionization potential and electron affinity. Softness, chemical potential, and electrophilicity are defined by the following formulas:

$$\chi \approx [IP + EA]/2, \quad \eta \approx [IP - EA]/2, \quad S = 1/2\eta, \quad \mu = -\chi, \quad \omega = \mu^2/2\eta\,.$$

Chemical reactivity parameters calculated by using the DFT/B3LYP method with 6-311G(d,p) basis set are given in Table 3. The χ, η, *S*, μ, and ω values of 5MF were calculated as 4.208 eV, 2.431 eV, 0.205 eV^{-1}, –4.208 eV, and 3.641 eV in the gas phase, respectively. Electronegativity is a chemical property that describes the ability of an atom or a functional group to attract electrons or electron density towards itself. The hardness is the ability of chemical system to resist the deformation of electron cloud under small perturbations encountered during the chemical process.

Conclusions. Assuming conformations of the 5MF molecule, we performed the conformational analysis by using the Spartan 08 software. We also made a potential surface scan on the dihedral angles between aldehyde and furan ring. We found two local minima (*cis*- and *trans*-rotamers) belonging to C_s symmetry. These two stable conformations are close in their energies. The fully optimized geometries at MP2 and DFT/B3LYP with 6-311G(d,p) basis sets were compared with the experimental and theoretical data. The evolution of the Raman and infrared spectra of 5MF was performed with theoretical and experimental data presented in the literature on the methyl, aldehyde, and furan. The *ab initio* MP2 and density func-

tional theory calculations reproduced the characteristics of the 5MF and are in good agreement with the experimental spectra recorded by Raman and infrared spectroscopy.

REFERENCES

1. A. J. Ragauskas et al., *Science*, **311**, 484 (2006).
2. J. N. Chheda, Y. R. Leshkov, and J. A. Dumesic, *Green Chem.*, **9**, 342–350 (2007).
3. M. Rose and R. Palkovits, *Macromol. Rapid Commun.*, **32**, 1299–1311 (2011).
4. G. W. Huber, S. Iborra, and A. Corma, *Chem. Rev*., **106**, 4044 (2006).
5. D. Vlachos, J. Chen, R. Gorte, G. Huber, and M. Tsapatsis, *Catal. Lett*., **140**, 77 (2010).
6. M. Bicker, J. Hirth, and H. Vogel, *Green Chem*., **5**, 280 (2003).
7. J. P. Lange, E. van der Heide, J. van Buijtenen, and R. Price, *Chem. Sus. Chem*., **5**, 150 (2012).
8. G. Allen and H. J. Bernstein, *Can. J. Chem*., **33**, 1055 (1955).
9. K. Dahlqvist and S. Forsen, *J. Phys. Chem*., **69**, 4020 (1965).
10. R. S. Abraham and T. M. Siverns, *Tetrahedron*, **28**, 3015–3024 (1972).
11. D. J. Chadwick, G. D. Meakins, and E. E. Richards, *Tetrahedron Lett*., **36**, 3183 (1974).
12. D. P. Roques, S. Combrisson, and F. Wehrli, *Tetrahedron Lett*., **12**, 104 (1975).
13. C. Petrongolo, *Chem. Phys. Lett*., **42**, 5–12 (1976).
14. I. G. Joh and L. Radom, *J. Am. Chem. Sot*., **100**, 3981 (1978).
15. T. S. Little, J. Qin, and J. R. Durig, *Spectrochim. Acta, A*, **45**, 789 (1989).
16. L. A. Montero, R. Jonte, L. A. Gonzalez, J. R. Diaz, and R. Alvarez Idaboy, *J. Phys. Chem*., **98**, 5607 (1994).
17. R. Crespo-Otero, L. A. Montero, G. Rosquete, J. A. Padron-Garcia, and R. H. Gonzalez-Jonte, *J. Comput. Chem*., **25**, 3 (2003).
18. F. A. Miller, W. G. Fateley, and R. E. Witkowski, *Spectrochim. Acta A*, **23**, 891–908 (1967).
19. R. A. Motiyenko, E. A. Alekseev, and S. F. Dyubko, *J. Mol. Spectrosc.*, **244**, 9–12 (2007).
20. *Spartan 08*, Wavefunction Inc., Irvine, CA 92612, USA (2008).
21. T. A. Halgren, *J. Comput. Chem*., **17**, 490–519 (1996).
22. *Gaussian 09*, Revision B.01, Gaussian Inc., Wallingford, CT (2010).
23. R. D. Dennington, T. A. Keith, and J. M. Millam, *GaussView 5*, Gaussian Inc. (2008).
24. A. D. Becke, *J. Chem. Phys*., **98**, 5648–5652 (1993).
25. *Modern Density Functional Theory: A Tool for Chemistry*, J. M. Seminario and P. Politzer (Eds.), **2**, Elsevier, Amsterdam (1995)
26. A. D. Becke, *J. Chem. Phys*., **107**, 8554–8560 (1997).
27. C. Lee, W. Yang, and R. G. Parr, *Phys. Rev. B*, **37**, 785–789 (1988).
28. W. J. Hehre, L. Random, P. V. R. Schleyer, and J. A. Pople, *Ab initio Molecular Orbital Theory*, Wiley, New York (1986).
29. M. A. Palafox, G. Tardajos, A. G. Martines, V. K. Rastogi, D. Mishra, S. P. Ojha, and W. Kiefer, *Chem. Phys*., **340**, 17 (2007).
30. N. C. Handy, P. E. Masley, R. D. Amos, J. S. Andrews, C. W. Murray, and G. Laming, *Chem. Phys. Lett*., **197**, 506 (1992).
31. *SQM version 2.0, Scaled Quantum Mechanical Force Field*, Green Acres Road, Fayetteville, Arkansas, USA (2013).
32. J. Baker, A. A. Jarzecki, and P. Pulay, *J. Phys. Chem. A*, **102**, 1412–1424 (1998).
33. D. Michalska and R. Wysokinski, *Chem. Phys. Lett*., **403**, 211 (2005).
34. T. Shalumova and J. M. Tanski, *Acta Cryst*., **E66**, 2266 (2010).
35. Ö. Dereli, S. Sudha, and N. Sundaraganesan, *J. Mol. Struct.*, **994**, 379–386 (2011).
36. D. Sajan, Y. Erdogdu, R. Reshmy, Ö. Dereli, K. Kurien Thomas, and I. Hubert Joe, *Spectrochim. Acta, A*, **82**, 118–125 (2011).
37. M. Arockia Doss et al., *Spectrochim. Acta, A: Mol. Biomol. Spectrosc.*, **151**, 773–784 (2015).
38. T. Kim, R. S. Assary, L. A. Curtiss, C. L. Marshall1, and P. C. Stair, *J. Raman Spectrosc*., **42**, 2069–2076 (2011).
39. T. Iliescu, F. D. Irimie, M. Bolboaca, C. Paisz, and W. Kiefer, *Vibr. Spectrosc.*, **29**, 235–239 (2002).

40. S. Subashchandrabose, H. SaleemY. Erdogdu, Ö. Dereli, V. Thanikachalam, and J. Jayabharathi, *Spectrochim. Acta, A*, **86**, 231–241 (2012).
41. F. J. Luque, J. M. Lopez, and M. Orozco, *Theor. Chem. Acc*., **103**, 343–345 (2000).
42. N. Okulik and A.H. Jubert, *Internet Electron. J. Mol. Des*., **4**, 17–30 (2005).
43. C. Parlak, M. Akdogan, G. Yildirim, N. Karagoz, E. Budak, and C. Terzioglu, *Spectrochim. Acta, A*, **79**, 263–271 (2011).
44. K. Fukui, *Science*, **218**, 747 (1982).
45. G. Gece, *Corros. Sci*., **50**, 2981–2992 (2008).
46. T. A. Koopmans, *Physica*, **1**, 104–113 (1933).